(275) (NO)

MSC INTERNAL NOTE NO. 64-EG-17

PROJECT APOLLO

ANALOG SIMULATION OF APOLLO BLOCK I CSM MANUAL THRUST VECTOR CONTROL FOR RETROFIRE IN EARTH ORBIT

Prepared by: Kenneth L. Lindsay
Kenneth L. Lindsay

Approved: Kenneth J. Cox
Kenneth J. Cox
Chief, Systems Analysis Branch

Approved: R. C. Chilton for
Robert C. Duncan
Chief
Guidance and Control Division

NATIONAL AERONAUTICS AND SPACE ADMINISTRATION
MANNED SPACECRAFT CENTER
HOUSTON, TEXAS
AUGUST 26, 1964

ANALOG SIMULATION OF APOLLO BLOCK I CSM MANUAL THRUST VECTOR CONTROL FOR RETROFIRE IN EARTH ORBIT

SUMMARY

An analog simulation of manual thrust vector control (TVC) of the Apollo Block I Command/Service Module (CSM) service propulsion system (SPS) for retrofire in earth orbit conducted by the Systems Analysis Branch is herein described. The mathematical model utilized consisted of the six-degree-of-freedom rigid-body equations of motion of the CSM and the equations of motion of two spring-mass systems (two translational degrees of freedom each) representing fuel and oxidizer slosh dynamics. Manual TVC is shown to be a feasible attitude control mode using either a proportional rate command or direct (acceleration) command system, proportional rate command being the more preferable from the viewpoints of handling quality and attitude control accuracy.

INTRODUCTION

Several manned earth orbital missions of the Apollo CSM are currently planned. Retrofire in earth orbit to initiate reentry for these missions will be effected by firing the SM main engine. At present, the retrofire maneuver consists of orienting the vehicle to a specified inertial attitude (either manually or automatically using the SM RCS), switching to the SPS automatic Δ V mode, and igniting the SM main engine. During main engine thrust, the vehicle attitude will be controlled by gimballing the engine automatically. The study described herein investigated the feasibility of a retrofire maneuver backup mode wherein main engine gimballing would be effected manually by the pilot. The objectives of the study were to:

a. Determine the feasibility of CSM manual thrust vector control with and without body rate damping (this involves application of rate command or acceleration command pilot control modes).

b. Determine the visual cues necessary for acceptable pilot control of retrofire.

c. Determine the accuracy with which the pilot can establish a specified ΔV vector under various conditions, such as initial thrust vector misalinement or initial body angular rates.

LIST OF SYMBOLS

A_1	scale factor for converting rotational hand controller pitch or yaw angles to commanded body angular rates in rate command mode, deg/sec-deg stick
A_2	scale factor for converting rotational hand controller pitch or yaw angles to commanded main engine gimbal angles in direct mode, deg/deg stick
$\Delta a_{X_{M_1}}, \Delta a_{Y_{M_1}}, \Delta a_{Z_{M_1}}$	components of acceleration due to thrust and fuel slosh along the X-, Y- and Z-axes respectively, ft/sec^2
$\Delta a_{X_{o_{M_1}}}, \Delta a_{Y_{o_{M_1}}}, \Delta a_{Z_{o_{M_1}}}$	components of acceleration due to thrust and fuel slosh along the X_o-, Y_o- and Z_o-axes respectively, ft/sec^2
B	angular off-set of main engine yaw gimbal about Z-axis, deg
C_1	fuel damping coefficient ($2\zeta\sqrt{K_1 m_1}$), lb/ft/sec
C_2	oxidizer damping coefficient ($2\zeta\sqrt{K_2 m_2}$), lb/ft/sec
D_x, D_y, D_z	components of distance from main engine gimbal point to combined center of mass along the X-, Y- and Z-axes respectively (positive from gimbal point along positive XYZ-axes), ft
$F_{X_{M_1}}, F_{Y_{M_1}}, F_{Z_{M_1}}$	components of external force on M_1 (excluding gravity) along the X-, Y- and Z-axes respectively, lb
h_1, h_2	depth of fuel and oxidizer, respectively, in tanks, ft
I_X, I_Y, I_Z	moments of inertia of M_1 about the X-, Y- and Z-axes respectively, slug-ft^2
$I_{y_{e_{h.p.}}}$	moment of inertia of main engine about axis through engine gimbal point parallel to Y-axis, slug-ft^2
$I_{z_{e_{h.p.}}}$	moment of inertia of main engine about axis through engine gimbal point parallel to Z-axis, slug-ft^2
K_1	spring constant of spring-mass system used to represent fuel slosh, lb/ft

K_2	spring constant of spring-mass system used to represent oxidizer slosh, lb/ft
K_p	gain in body rate feedback loop of CSM RCS electronics, deg/deg/sec
K_R	rate gain in manual TVC system, deg/deg/sec
K_ϕ	gain in roll attitude feedback loop of CSM RCS electronics, deg/deg
K_{δ_Q}	gain in attitude feedback loop of main engine pitch gimbal servomechanism, deg/deg
$K_{\dot{\delta}_Q}$	gain in rate feedback loop of main engine pitch gimbal servomechanism, deg/deg/sec
K_{δ_R}	gain in attitude feedback loop of main engine yaw gimbal servomechanism, deg/deg
$K_{\dot{\delta}_R}$	gain in rate feedback loop of main engine yaw gimbal servomechanism, deg/deg/sec.
L_X, L_Y, L_Z	external torques on M about the X-, Y- and Z-axes respectively, ft-lb.
L_{X_J}	RCS control torque on M_1 about X-axis, ft-lb
l_e	distance from main engine gimbal point to main engine c.g.; ft
l_{X_1}, l_{Y_1}, l_{Z_1}	components of distance from main engine gimbal point to m_1 along X-, Y- and Z-axes respectively (positive from gimbal point along positive XYZ-axes), ft
l_{X_2}, l_{Y_2}, l_{Z_2}	components of distance from main engine gimbal point to m_2 along X-, Y- and Z-axes respectively (positive from gimbal point along positive XYZ-axes), ft
M_1	total vehicle mass, excluding m_1 and m_2, slugs
M_e	mass of main engine, slugs
m_1	sloshing portion of fuel mass, slugs
m_2	sloshing portion of oxidizer mass, slugs
m_{f_t}	total fuel mass in tank, slugs

m_{o_t}	total oxidizer mass in tank, slugs
p, q, r	components of vehicle angular velocity about the X-, Y- and Z-axes respectively, rad/sec
r_1, r_2	radii of fuel and oxidizer tanks respectively, ft
S	complex variable
T	thrust of main engine, lb
$\Delta V_{X_{O_{M_1}}}$, $\Delta V_{Y_{O_{M_1}}}$, $\Delta V_{Z_{O_{M_1}}}$	components of velocity of M_1 due to external forces on M_1 (excluding gravity) along X_o, Y_o and Z_o-axes respectively, ft/sec
X, Y, Z	vehicle body axes having origin at center of mass with X-axis positive through command module nose, Y-axis positive out pilot's right arm, Z-axis completing right-handed system
X_o, Y_o, Z_o	inertial axis system having X_o-axis along desired delta-V vector, Y_o-axis normal to orbit plane and Z_o-axis completing right-handed coordinate system.
λ_{y_1}, λ_{z_1}	components of displacement of m_1 relative to M_1 along the Y- and Z-axes respectively, ft
λ_{y_2}, λ_{z_2}	components of displacement of m_2 relative to M_1 along the Y- and Z-axes respectively, ft
θ, Ψ, ϕ	Euler angles defining orientation of XYZ-triad relative to $X_o Y_o Z_o$-triad (θ, Ψ, ϕ rotation sequence), deg
δ_Q	main engine pitch gimbal angle, measured positive clockwise when viewed along negative Y-axis, deg
$(\delta_R - B)$	main engine yaw gimbal angle, measured positive clockwise when viewed along negative Z-axis, deg
ξ	Root of Bessel function of first kind, order one, dimensionless
ζ	fuel or oxidizer damping ratio

Note: A dot over a variable represents a time rate of change of that variable.

DESCRIPTION OF SIMULATION

Characteristics of Simulated Vehicle

The vehicle considered was an Apollo Block I CSM having one fuel tank and one oxidizer tank empty, the remaining two tanks containing 12.5% of their original fuel and oxidizer respectively. The physical characteristics of the vehicle are listed in Table I.

Equations of Motion

The six-degree-of-freedom equations of motion of the vehicle were programed on the analog computer. The equations included the effects of engine inertia reaction (tail-wags-dog) and fuel and oxidizer sloshing on vehicle dynamics.

The equations of motion were derived utilizing the following assumptions:

(1) Constant total mass

(2) Products of inertia neglected

(3) The damping ratio (ζ) for each sloshing mass assumed to be 0.005 of critical.

(4) Only the fundamental sloshing modes significant (all higher modes assumed negligible).

(5) Fluid is non-viscous, incompressible, and irrotational.

(6) Fuel and oxidizer masses constant (zero rate of change of fuel or oxidizer level in tanks).

(7) All propellants settled at tank bottoms during a previous ullage maneuver.

(8) Tanks are cylindrical, flat bottomed, and circular in cross-section.

(9) Sloshing masses represented by equivalent spring mass systems.

Formulae presented in Table II (obtained from reference 1) were used to compute the propellant sloshing parameters. These equations were developed from hydrodynamic theory by comparing the equations of motion of a fluid described in assumption (5) above in a tank described

in assumption (8) above to the equations of motion of a spring mass system mounted inside a rigid tank. These parameters permit the fluid slosh to be represented by a less complicated mathematical model.

The complete system of equations programed on the analog computer is shown in block diagram form in figure 1. The axis systems employed are also shown in figure 1.

Control System

Attitude about the roll axis was controlled by the RCS operating in the attitude hold mode. Attitude control in pitch and yaw was effected manually by means of a rotational hand controller driving the CSM main engine gimbal servomechanisms. The servomechanisms were represented by second-order proportional systems having an overall frequency of 20 rad/sec with a damping of 0.7 of critical. The only nonlinearities simulated were limiters on gimbal angles, velocities, and accelerations. The pitch-axis gimbal travel was limited to ± 6 degrees and the yaw-axis gimbal travel limited to ± 8.5 degrees. Gimbal rate about both axes was limited to ± 17.19 deg/sec and gimbal acceleration about both axes limited to ± 172 deg/sec^2. Gimbal actuator clutch dynamics and nonlinear gimbal rate feedback gains of the actual vehicle were not included.

Simulator Cockpit

The simulator cockpit used in this simulation is shown in figure 2. The command astronaut's chair is a C-119 pilot's chair, the hand controller a prototype Gemini rotation controller having a maximum deflection about the pitch, yaw, or roll axis of ± 10 degrees. The controller was spring loaded to return to its null position when released.

The pilot display panel shown in figure 2 included the following instruments:

(1) FDAI (attitude indicator)

(2) 21-inch cathode ray tube for simulated landmark (out-the-window display)

(3) Thrust ignition and cutoff switch

(4) Mode select switch (direct or rate command)

(5) Hand controller

(6) Clock with sweep second hand

TEST PROCEDURE

All simulated retrofire maneuvers began with the vehicle oriented such that the main engine thrust vector ($\overline{T}$) was approximately oriented along the desired ΔV vector. The initial engine gimbal trim angles (δ_{Q_T} and δ_{R_T}) were such that the thrust vector did not always point exactly through the center of mass. To initiate a run, the pilot pressed the thrust ignition and cutoff button on the display panel to ignite the main engine and attempted to hold the vehicle at the desired attitude by observing either the pitch and yaw attitude error needles or the simulated landmark and varying the thrust vector orientation by means of the hand controller. After a specified time (obtained from sweep second-hand clock on display panel), the pilot terminated the thrust by again pressing the thrust ignition and cutoff button on the panel.

Pilot performance was measured by comparing the magnitude and direction of the desired ΔV vector to the magnitude and direction of the achieved ΔV vector.

RESULTS

The analog runs in this study were made to evaluate manual capability to perform an earth orbit retrofire maneuver using the SPS main engine for pitch and yaw attitude control. Personnel from the Astronaut Office and FCSD participated in the simulation. Among the astronauts who "flew" the simulation were Neil Armstrong, James McDivitt, Elliot See, Edward White, and Russell Schweickart. The FCSD personnel participating were H. E. Smith and J. F. Stegall. The numerical results presented in this report were obtained from runs made by Mr. Stegall, although the conclusions reached from the simulation were based on the performance of all of the above personnel. Pilot performance was evaluated by determining the magnitude of the cross-axis velocity after 15 seconds of thrusting, corresponding to a total ΔV of 435 feet/second imparted to the spacecraft. The runs made during the study were divided into four grups which were to evaluate pilot performance: (1) using proportional rate command and acceleration command control modes for attitude control, (2) using different controller sensitivity in the acceleration mode, (3) in the presence of various initial pitch and yaw thrust misalinement, and (4) using different visual cues.

The initial conditions for the four groups of representative runs are contained in tables III, IV, and V. Although the initial misalinements used in some of the runs were considerably greater than any likely to occur during an actual maneuver, they were included to obtain an index of pilot capability under worst case conditions. The results of this study are also contained in tables III, IV, and V as well as in time histories of selected parameters for representative runs. The quantities θ, ψ, and ϕ in the time histories are the vehicle pitch, yaw, and roll Euler angles, respectively, relative to an inertial axis system having the X_O-axis along the desired ΔV vector, the Y_O-axis normal to the orbit plane, and the Z_O-axis completing the right-handed system. The quantities ΔV_{Y_O} and ΔV_{Z_O} are components of velocity due to thrust along the Y_O- and Z_O-axes, respectively.

Comparison of Rate and Acceleration Command Modes

The data of table III indicate the pilots were able to perform the retrofire maneuver without excessive cross-axis velocity error even in the presence of severe center-of-gravity thrust misalinements. The spacecraft was always brought under control in the rate command mode, but this was not necessarily the case for the acceleration command control mode. However, even though the vehicle was not always brought completely under control after 15 seconds of thrusting using the acceleration command mode, the largest cross-axis velocity error acquired in any of the runs listed in table III was only 70 feet/second. The time history of vehicle attitude and cross-axis velocity components for the run from which this result was obtained (Run 50) is shown in figure 3. For the purpose of comparing the relative handling qualities of the vehicle in the rate command and acceleration command modes, the time history of the same quantities obtained using the rate command mode for the same initial conditions (Run 49) is also included in figure 3. As evidenced by the time history of θ and ψ, the vehicle is much easier to control in the rate command mode. In fact, as mentioned above, the vehicle was not brought completely under control in the acceleration command mode, as again evidenced by the time history of θ and ψ. Nevertheless, the oscillatory behavior of these quantities indicates that the pilot was able to exercise modest control over the vehicle for the required 15 seconds.

Effect of Varying Hand Controller Sensitivity

Another series of runs were made using the acceleration command mode to determine the effect of varying controller sensitivity (degrees gimbal commanded/degree hand controller deflection) on cross-axis velocities and handling qualities of the vehicle. The initial conditions, controller sensitivity, and resultant cross-axis velocity error after 15 seconds of thrusting for a group of these runs are shown in table IV. For each run, the thrust vector was initially misalined one degree in both pitch and yaw with the roll axis in an attitude-hold mode. The controller sensitivity was varied from 0.4 to 1.6 deg gimbal/deg stick. While the cross-axis velocity error after 15 seconds of thrusting varied from zero to 16 ft/sec over the range of controller sensitivities investigated, no definite trend was established; i.e., the cross-axis velocity error did not increase uniformly with increasing controller sensitivity. However, a definite trend was established insofar as handling quality of the vehicle was concerned. This is illustrated in figures 4 through 7. Although the maximum pitch and yaw excursions did not increase significantly with increasing controller sensitivity, the engine maximum gimbal positions (δ_Q about pitch axis, δ_R about yaw axis), velocities and accelerations increased steadily with increasing controller sensitivity, thus indicating an increasing pilot tendency to "over-control" the vehicle as controller sensitivity increases.

Effect of Initial Thrust Misalinements

The third group of runs was made using the acceleration command mode to determine the effect of a range of initial thrust misalinements on cross-axis velocity error. The initial pitch and yaw thrust misalinements and resultant cross-axis velocity errors after 15 seconds of thrusting for a representative group of runs in this series are shown in table V. Thrust misalinements were varied from -4.67 to +7.33 degrees in yaw and from -4.83 to +5.17 degrees in pitch. The cross-axis velocity errors resulting ranged from 15 to 57 ft/sec using a controller sensitivity of 0.8 deg gimbal/deg of stick deflection. No definite trend of cross-axis velocity error with initial thrust misalinement is apparent from these runs. The cross-axis velocity error for these short runs depends largely on the pilot response to the initial transient; however, it is believed that a statistical analysis would reveal a trend of increasing error with increasing initial thrust misalinement. No attempt was made in the present simulation to obtain statistical data or to separate out learning trends.

Effect of Visual Cues

A comparison of pilot performance was made for the maneuver using (1) an FDAI and (2) an out-the-window display for attitude information. The equipment used to simulate an out-the-window display was the 21-inch cathode ray tube (CRT) shown in figure 2. The line which can be seen near the center of the CRT simulated a landmark on the surface of the earth. The signals used to drive the landmark were the same as those used to drive the attitude error needles of the FDAI (the pitch and yaw Euler angles projected onto body axes). Since the CRT was physically larger than the FDAI, the resolution on the CRT was considerably better. In addition, the line simulating the landmark was believed to be considerably more distinct on the CRT than an actual landmark as viewed from the spacecraft would appear because of clouds, other objects in the vicinity of the landmark, etc. For these reasons the data obtained using the simulated landmark for attitude reference are considered to be questionable in validity and are not presented in this report.

CONCLUSIONS

Based on the analysis of the data obtained from this study, the following conclusions can be made:

a. Manual thrust vector control of the Apollo Block I CSM for a retrofire maneuver is feasible.

b. The rate command mode is preferable to the acceleration command mode, although either mode is acceptable.

REFERENCES

1. North American Aviation, Inc. Inter-office letter dated December 12, 1962, to E. F. Dudek. Preliminary estimates of Service Module Propellant Sloshing Parameters, by M. W. Kishi.

TABLE I

Constants

Quantity	Valve
A_1	2 rad/sec-rad stick
A_2	0.4 - 1.6 rad/rad stick
B	4 deg
C_1	0.7154
C_2	1.483
D_x	9.17 ft
D_y	.533 ft
D_z	.133 ft
I_x	13,500 slug-ft^2
I_y	45,500 slug-ft^2
I_z	45,500 slug-ft^2
K_ϕ	1 rad/rad
$K_{\dot{\varepsilon}_q}$	28 rad/sec
K_{ε_q}	400 rad^2/sec^2
$K_{\dot{\varepsilon}_r}$	28 rad/sec

(Table I - continued)

K_{δ_r}	400 rad^2/sec^2
K_p	0.25 rad/rad/sec
K_r	1.5 rad/rad/sec
K_1	382 lb/ft
K_2	743 lb/ft
L_{x_j}	1282 ft-lb
l_{x_1} -D_x	-7.7 ft
l_{y_1} -D_y	-1.93 ft
l_{z_1} -D_z	3.96 ft
l_{x_2} -D_x	-7.75 ft
l_{y_2} -D_y	3.4 ft
l_{z_2} -D_z	2.8 ft
$m_e l_e$	33.3 slug-ft
m_1	13.4 slugs
m_2	29.6 slugs
M_1	752 slugs
$I_{Y_{e_{h.p.}}}$	300 $slug\text{-}ft^2$
$I_{Z_{e_{h.p.}}}$	300 $slug\text{-}ft^2$
T_o	21,900 lb

TABLE II

Propellant Sloshing Parameters

$$m_1 = \frac{2 m_{f_T} \tanh(\xi h_1/r_1)}{\xi(h_1/r_1)(\xi^2-1)}$$

$$k_1 = \frac{\left[2 m_{f_T} \tanh(\xi_1 h_1/r_1)\right] T/(M_1+m_1+m_2)}{h_1(\xi^2-1)}$$

$$m_2 = \frac{2 m_{o_T} \tanh(\xi h_2/r_2)}{\xi(h_2/r_2)(\xi^2-1)}$$

$$k_2 = \frac{\left[2 m_{o_T} \tanh(\xi h_2/r_2)\right] T/(M_1+m_1+m_2)}{h_2(\xi^2-1)}$$

TABLE III

Comparison of Rate Command and Acceleration Command Modes in Pitch and Yaw for Various Initial Roll Rates and Thrust Misalignments*

Run No.	Control Mode, Pitch and Yaw Axes	Control Mode Roll Axis	Thrust Misalignment Yaw Axis (Deg)	Thrust Misalignment Pitch Axis (Deg)	Initial Roll Rate (Deg/Sec)	Resultant Cross-Axis Velocity Error after 15 sec of Thrusting (ft/sec)
39	Rate Command	Uncontrolled	0	0	1	30
40	Accel.Command	"	"	"	"	40
41	Rate Command	"	"	"	5	20
42	Accel. Command	"	"	"	"	30
43	Rate Command	"	"	"	10	0
44	Accel. Command	"	"	"	"	10
47	Rate Command	"	7.8	"	1	40
48	Accel. Command	"	"	"	"	30
49	Rate Command	"	"	"	5	30
50	Accel. Command	"	"	"	"	70
52	Rate Command	"	"	"	10	0
53	Accel. Command	"	"	"	"	10
54	Rate Command	"	"	3.2	1	40
55	Accel. Command	"	"	"	"	50
56	Rate Command	"	"	"	5	30
57	Accel. Command	"	"	"	"	50
58	Rate Command	"	"	"	10	0
59	Accel. Command	"	"	"	"	20

*(1) Vehicle is initially oriented in desired direction for retrofire maneuver with zero pitch and yaw rate.

(2) Pitch and Yaw controller sensitivity is 1.72 (deg/sec)/(deg stick) in rate command mode and 0.6 (deg gimbal)/(deg stick) in pitch and 1.25 (deg gimbal)/(deg stick) in yaw in acceleration command mode.

TABLE IV

Effect of Controller Sensitivity on Cross-Axis Velocity Errors in Acceleration Command Mode*

Run No.	Control Mode, Roll Axis	Thrust Misalignment, Yaw Axis (Deg)	Thrust Misalignment, Pitch Axis (Deg)	Controller Sensitivity Pitch & Yaw Axes (Deg Gimbal/ Deg Stick)	Resultant Cross-Axis Velocity Error After 15 Sec of Thrusting (ft/sec)
200	Attitude Hold	1.0	1.0	0.4	5
201	"	"	"	"	3
202	"	"	"	"	0
203	"	"	"	"	5
204	"	"	"	"	5
205	"	"	"	0.8	8
206	"	"	"	"	4
207	"	"	"	"	2
208	"	"	"	"	5
209	"	"	"	"	1
210	"	"	"	1.2	5
211	"	"	"	"	8
212	"	"	"	"	7
213	"	"	"	"	13
214	"	"	"	"	16
215	"	"	"	1.6	16
216	"	"	"	"	9
217	"	"	"	"	5
218	"	"	"	"	15
219	"	"	"	"	10

*Vehicle is initially oriented in desired direction for retrofire maneuver with zero angular rate.

TABLE V

Effect of Thrust Misalignment on Cross-Axis Velocity Errors in Acceleration Command Mode*

Run No.	Control Mode Roll Axis	Thrust Misalignment, Yaw Axis (Deg)	Thrust Misalignment, Pitch Axis (Deg)	Controller Sensitivity, Pitch & Yaw Axes (Deg Gimbal/ Deg Stick)	Resultant Cross-Axis Velocity error after 15 sec of Thrusting (ft/sec)
220	Attitude Hold	1.33	5.17	0.8	40
222	"	3.33	3.17	"	18
223	"	5.33	1.17	"	20
224	"	-2.67	1.17	"	40
225	"	5.33	3.17	"	22
226	"	-4.67	1.17	"	25
230	"	3.33	-4.83	"	48
231	"	1.33	-2.83	"	18
232	"	7.33	-4.83	"	57
233	"	3.33	-2.83	"	15
234	"	1.33	-4.83	"	18
235	"	-4.67	-2.83	"	54
236	"	-4.67	-4.83	"	47
237	"	1.33	-2.83	"	17
238	"	-2.67	-4.83	"	46

*Vehicle is initially oriented in the desired direction for retrofire maneuver with zero angular rate.

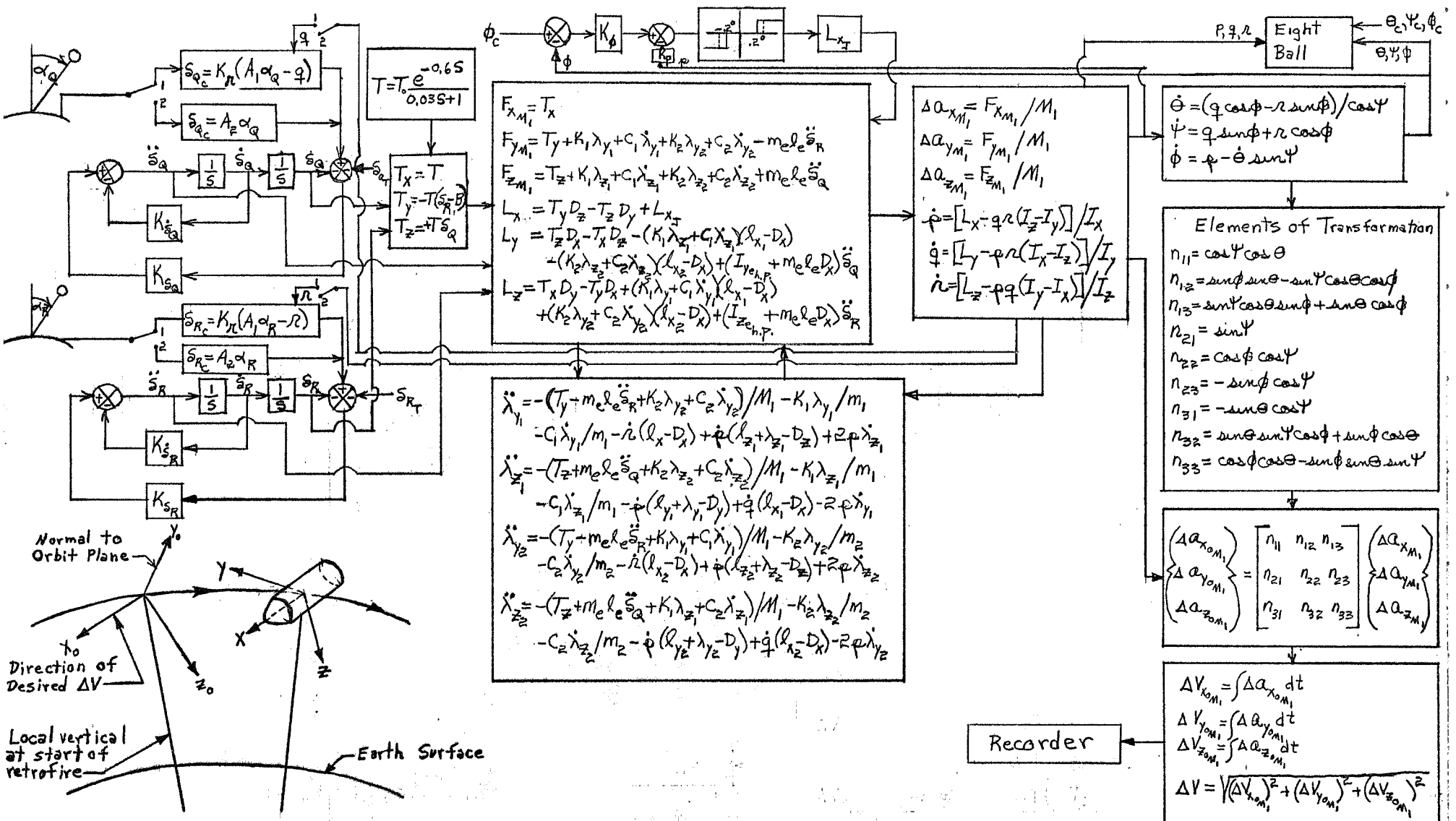

Figure 1: CSM Manual TVC Mathematical Model

NASA
S-64-26646

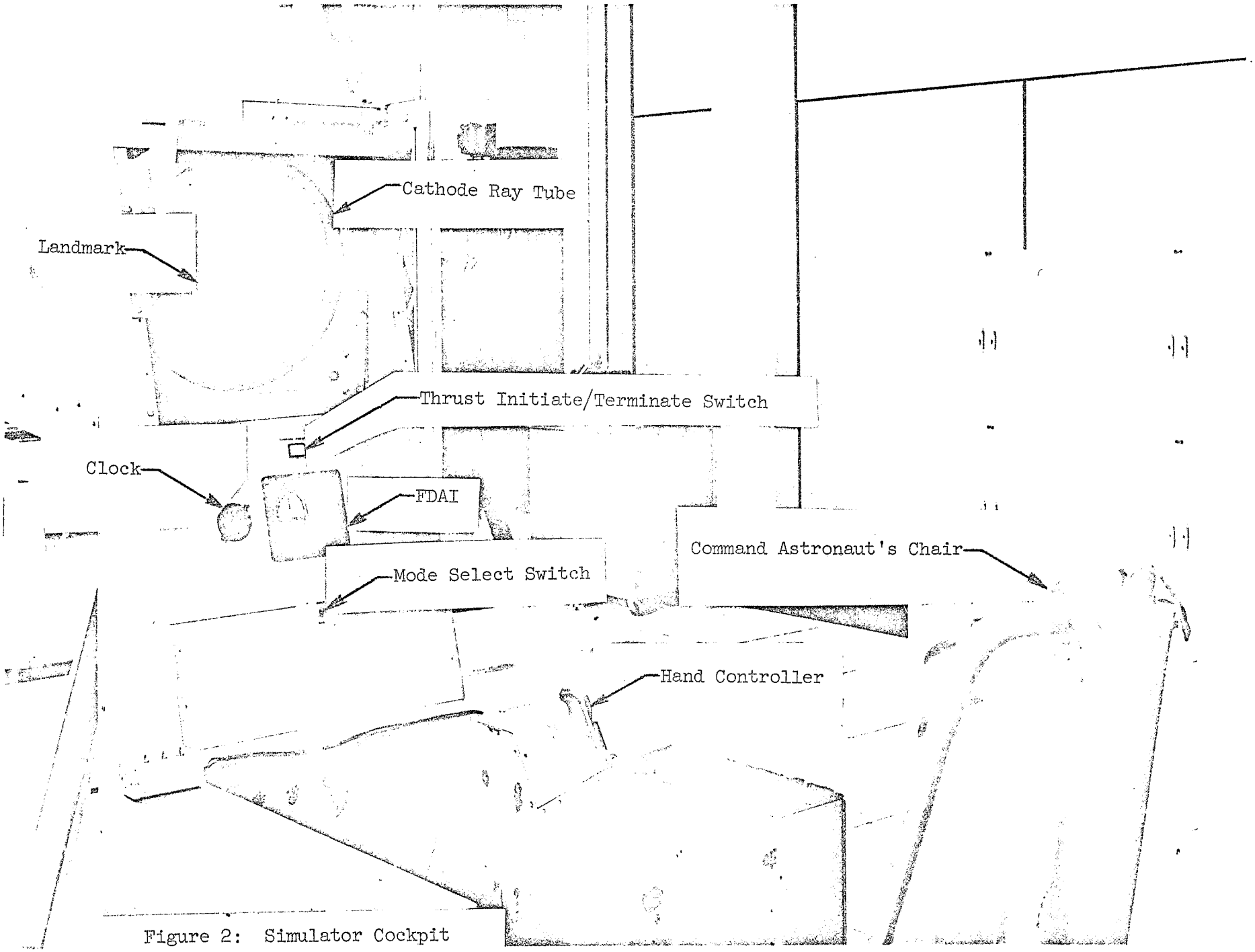

Figure 2: Simulator Cockpit

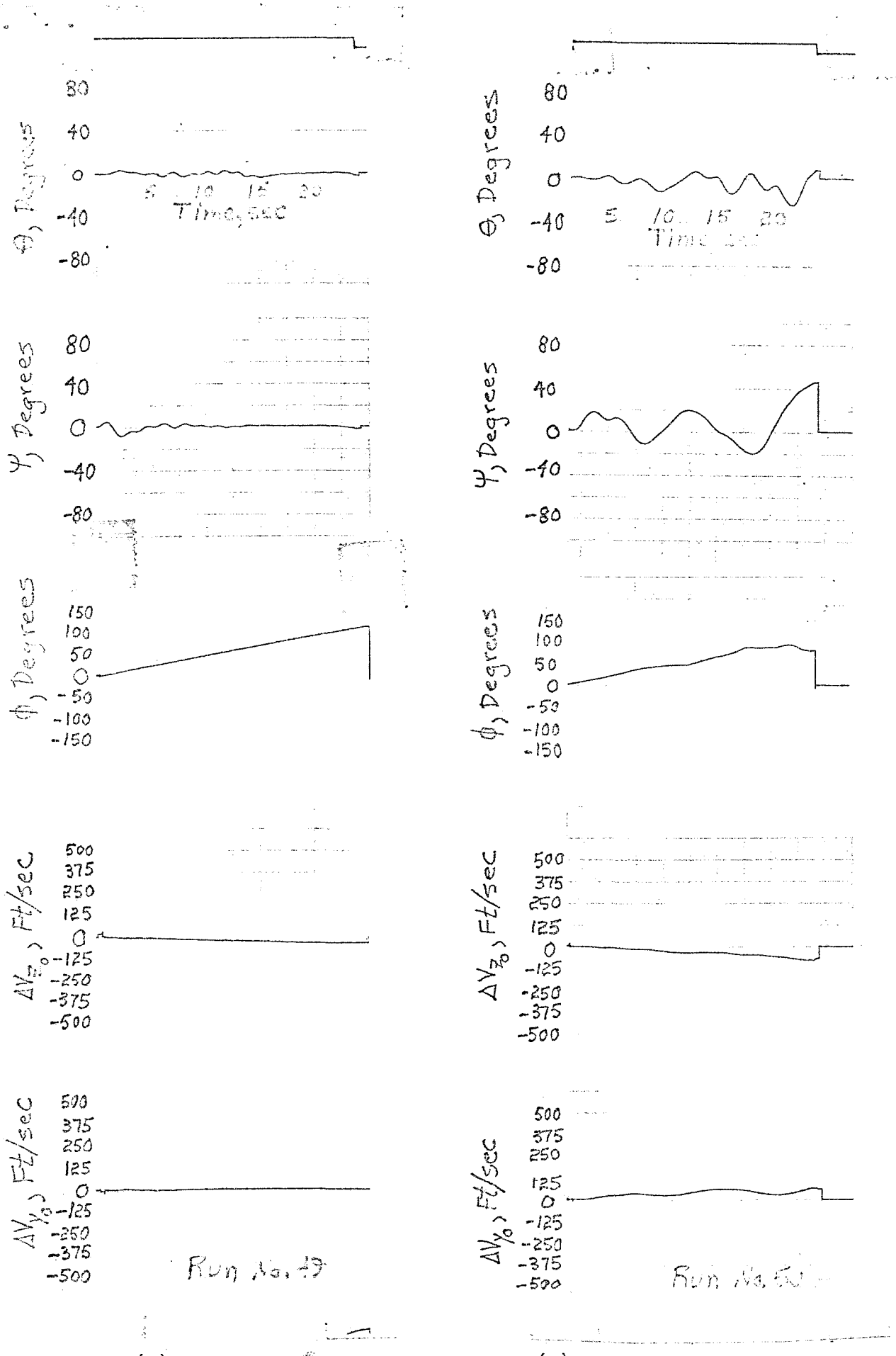

(a) Rate Command

(b) Acceleration Command

Figure 3: Comparison between rate command and acceleration command modes for typical retrofire maneuver

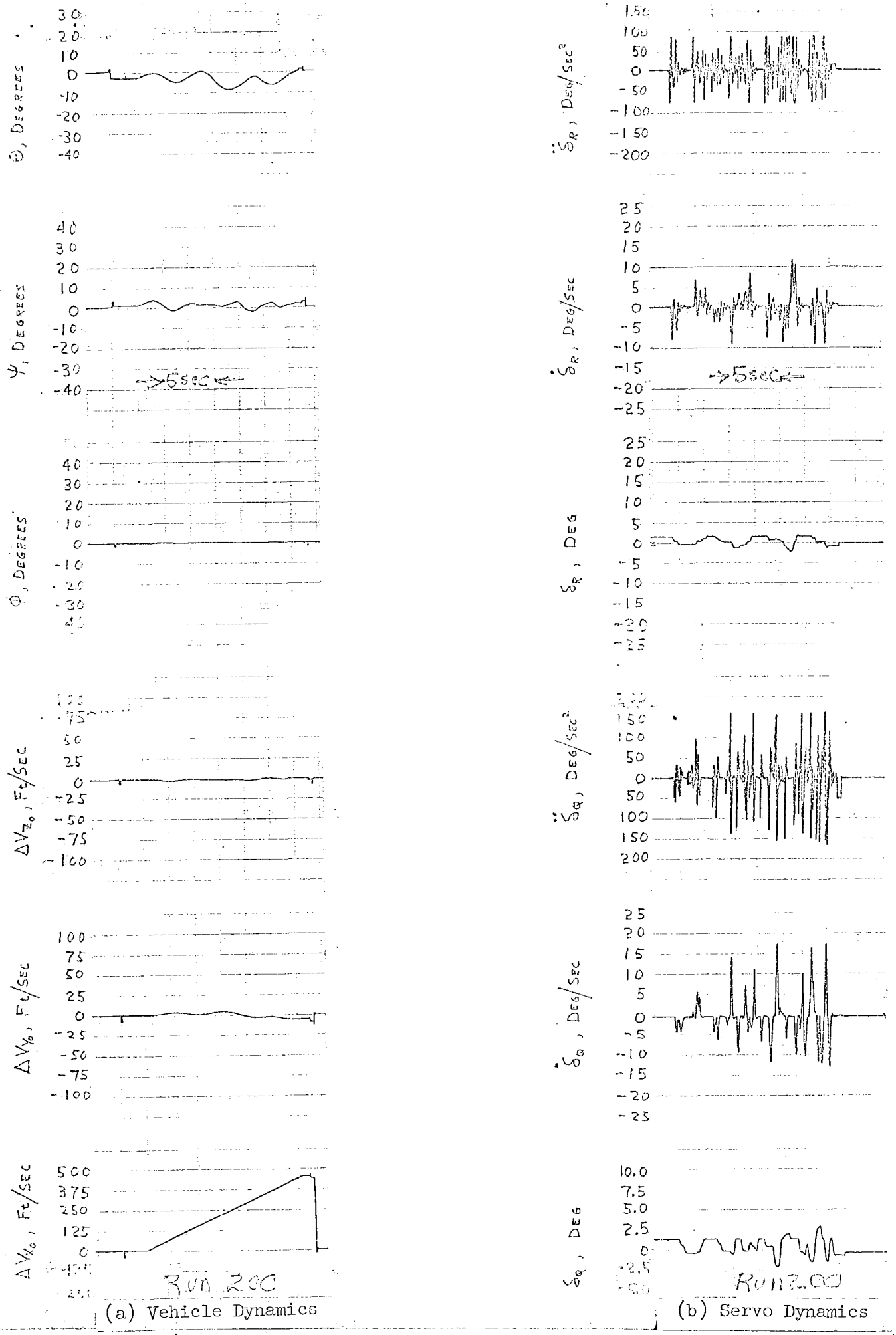

(a) Vehicle Dynamics

(b) Servo Dynamics

Figure 4: Typical time history of vehicle and servo dynamics using acceleration command mode with stick authority of 0.4 deg gimbal/deg stick.

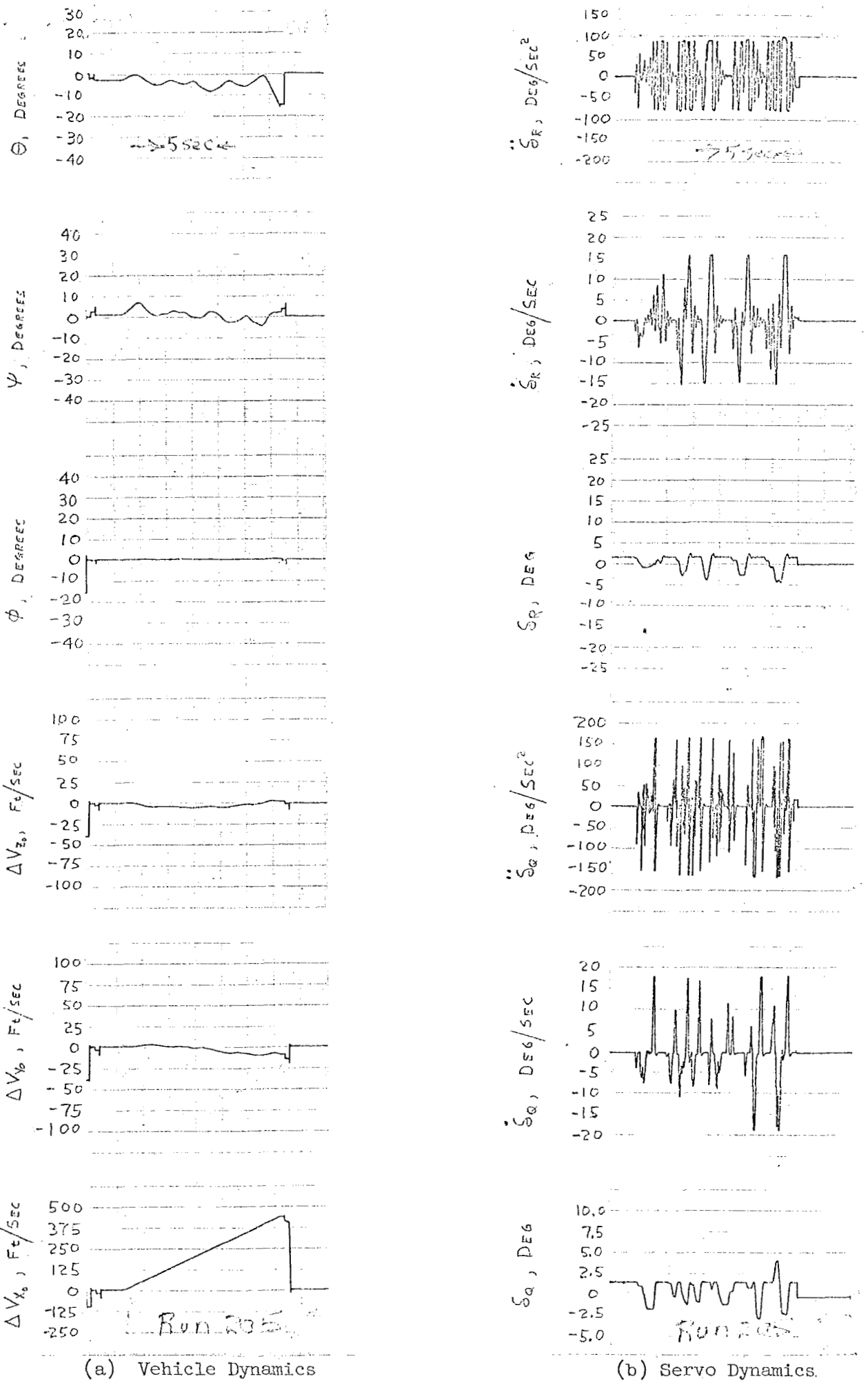

(a) Vehicle Dynamics

(b) Servo Dynamics

Figure 5: Typical time history of vehicle and servo dynamics using acceleration command mode with stick authority of 0.8 deg gimbal/deg stick.

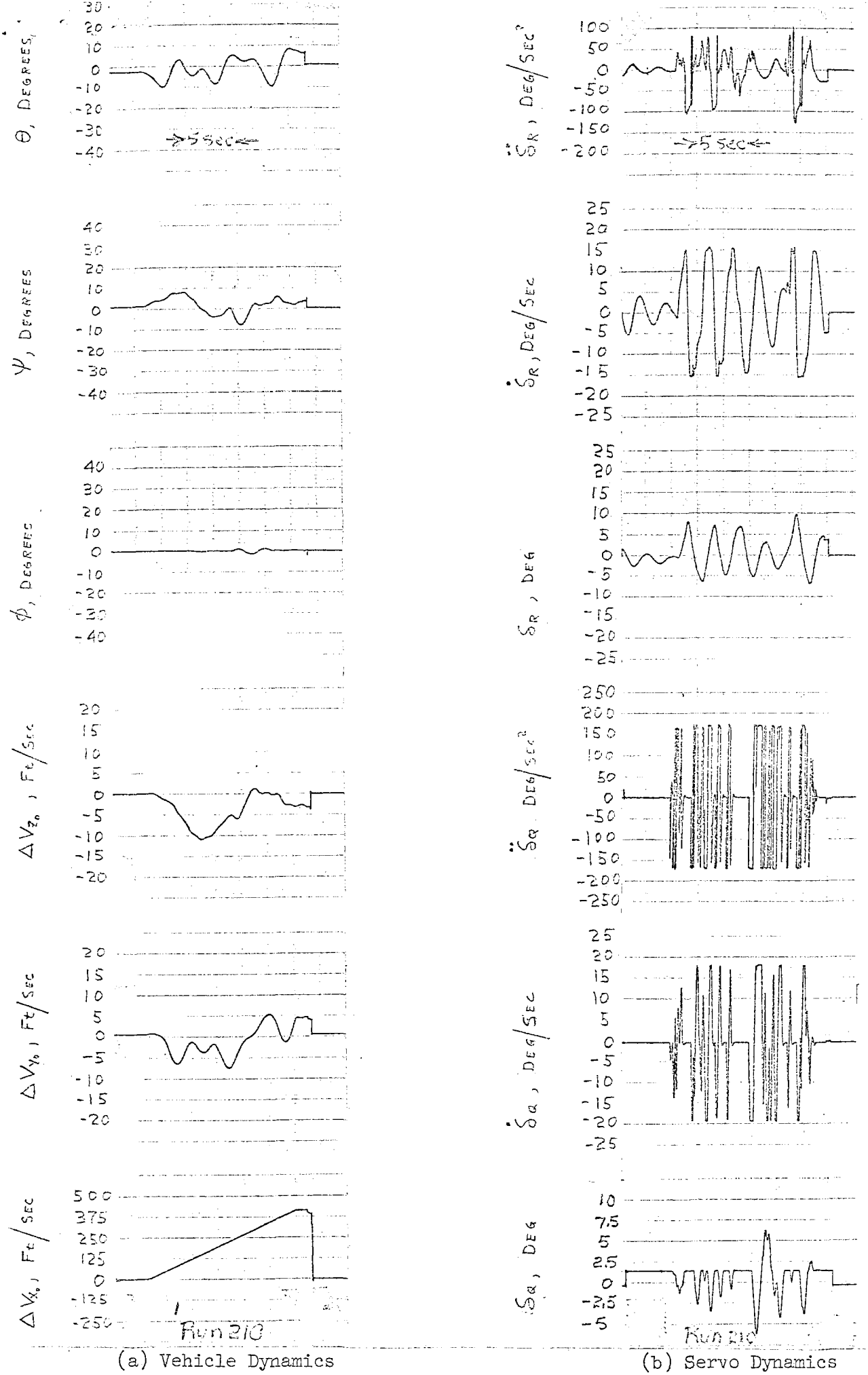

(a) Vehicle Dynamics

(b) Servo Dynamics

Figure 6: Typical time history of vehicle and servo dynamics using acceleration command mode with stick authority of 1.2 deg gimbal/deg stick.

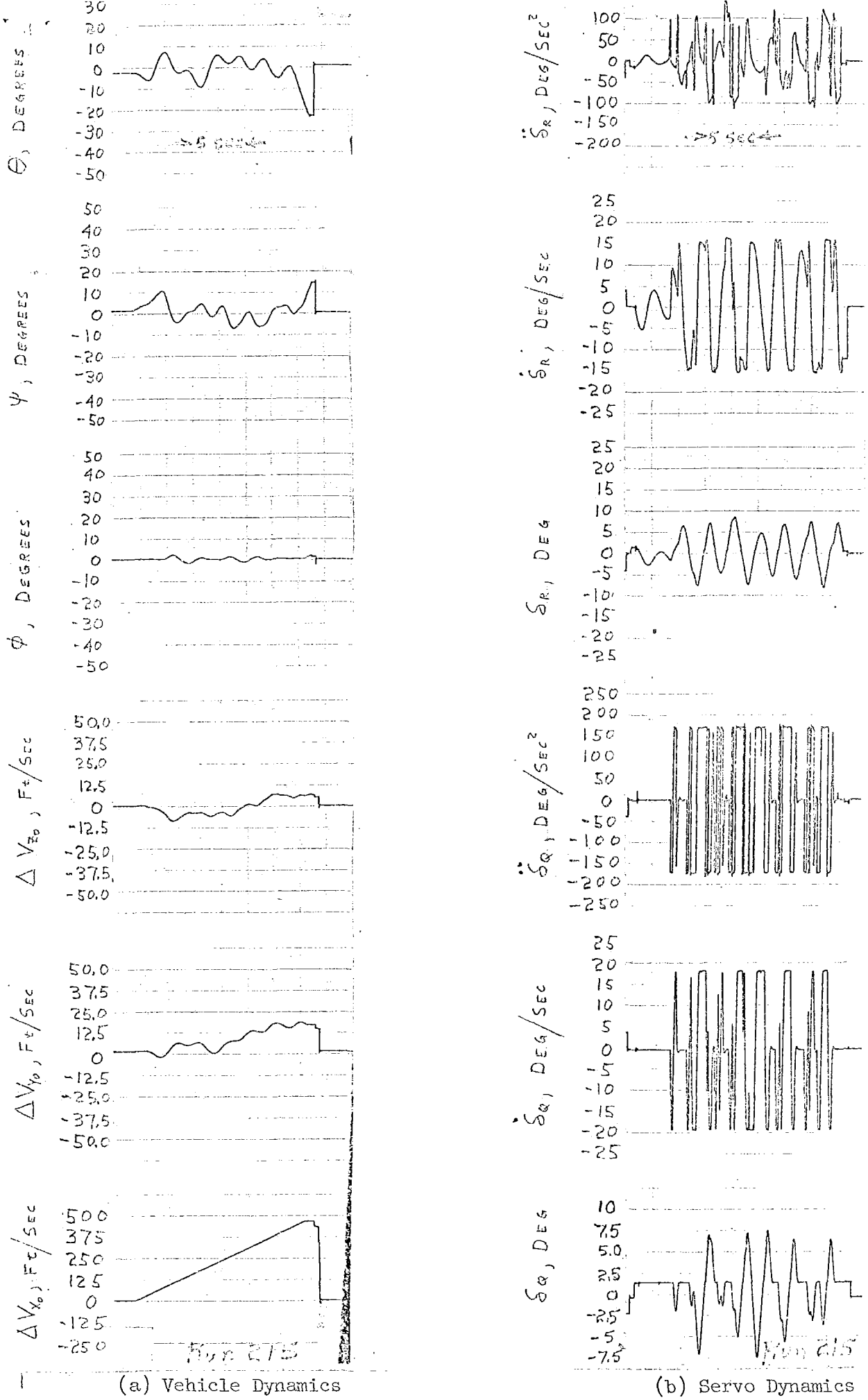

(a) Vehicle Dynamics

(b) Servo Dynamics

Figure 7: Typical time history of vehicle and servo dynamics using acceleration command mode with stick authority of 1.6 deg gimbal/deg stick.